Fabrication of nanofibres via polyvinylpyrrolidone by sol–gel method and electro-spinning technique

Zhaobing Cai, Guo Jin, Xuifang Cui, Wei Zheng, Erbao Liu, Yang Wang, Na Tan

Key Laboratory of Superlight Material and Surface Technology of Ministry of Education, College of Material Science and Chemical Engineering, Institute of Surface/Interface Science and Technology, Harbin Engineering University, Harbin 150001, People's Republic of China
E-mail: jinjg721@163.com

Published in Micro & Nano Letters; Received on 8th October 2014; Accepted on 29th October 2014

ZrO_2 fibres have been used in aspects of aeronautics and astronautics because of their properties such as high strength, good toughness and thermal shock resistance. In this reported work, polyvinylpyrrolidone (PVP)/$Y(NO_3)_3{\cdot}6H_2O$/$ZrOCl_2{\cdot}8H_2O$ (PVP-precursor) nanofibres were prepared by the sol–gel method and an electro-spinning technique. Then, the ZrO_2 fibres by Y-doping were obtained by calcination of the above precursor fibres at 550°C for 0.5 h. These fibres were characterised by X-ray diffraction, scanning electron microscopy, energy-dispersive X-ray spectroscopy, Fourier transform infrared spectroscopy, differential scanning calorimetry and thermogravimetry to study the physical and chemical properties. The formation mechanism of ZrO_2 fibres is also illustrated. The results show that: (i) the diameter of the nanofibres is in the range of 500–3000 nm; (ii) PVP-precursor fibres should reach the level of obvious dehydration, oxidation decomposition and phase transition to synthesise ZrO_2 nanofibres; (iii) through thermal poly-condensation reaction, PVP turns into a network structure of graphitised carbon.

1. Introduction: ZrO_2 fibres are the ideal insulation materials to bear ultra-high temperatures under extreme conditions, as they have high strength [1], good toughness [2] and thermal shock resistance [3]. Owing to these features they have been used in aspects of aeronautics and astronautics. As is known, the main preparation methods of ZrO_2 fibres and products are the solution impregnation method [4, 5], the sol–gel method [6, 7], electrostatic spinning method [8, 9]. Among these three methods, the electrostatic spinning method, considered as a very simple and efficient method to make nanofibres, has so many advantages, like high repeatability, simple and convenient operating process and adjustable fibre size [10].

Various types of nanofibres such as polymer fibres, biological macromolecular fibres and inorganic nanometre fibres can be fabricated by electrostatic spinning. Polyvinyl alcohol, polyvinyl acetate, polyvinylpyrrolidone (PVP), polyethylene oxide and so on can be used in electrostatic spinning. Owing to the low toxicity, good physiological intermiscibility, strong expansion performance and excellent solubility in water and organic solvents, PVP is widely applied in electrostatic spinning domain. At the same time, polymer/inorganic composite fibres can be the precursor, then inorganic nanofibres are synthesised by burning-off the polymer, which is relatively simple and easy to control, arousing the attention of an increasing number of researchers [8, 9, 11–13].

Researches on the preparation of ZrO_2 fibres by the electrostatic spinning method have been carried out for many years. Unfortunately, the major researches were just to test the physical and chemical properties of synthetic fibres. The mechanism of electrostatic spinning for the mechanism of zirconia nanofibres has been less reported. With the sol–gel method and the electrostatic spinning technique, Y-doping ZrO_2 composite fibres were synthesised using PVP as the precursor solvent. The emphasis was on the physical and chemical properties of composite nanofibres as well as the preliminary investigation of the mechanism of zirconia nanofibres.

2. Experimental: $Y(NO_3)_3{\cdot}6H_2O$ and $ZrOCl_2{\cdot}8H_2O$ were used as starting materials. In our research, about 1:1 molar ratio of Zr/Y was maintained. First, $Y(NO_3)_3{\cdot}6H_2O$ and $ZrOCl_2{\cdot}8H_2O$ were mixed in a beaker, then dissolved in a certain amount of deionised water by hand stirring. After $Y(NO_3)_3{\cdot}6H_2O$ and $ZrOCl_2{\cdot}8H_2O$ were absolutely dissolved, the mixture solution was clear; this was then followed by the addition of PVP. Subsequently, the mixture was magnetically stirred at room temperature for several hours until it became clear and transparent. After a period of time standing, the mixture was added to the equipment of the electrostatic spinning to obtain the composite fibres of the PVP precursor. The collected composite fibres of PVP the precursor were calcined from room temperature to 550°C with a heating rate of 5°C/min and remained for 0.5 h.

The schematic diagram of the electrostatic spinning device is shown in Fig. 1. The device was made up of a push-type injection pump, an injection syringe, a high-voltage power supply and a collector. The collector, which was earthed, laid a layer of aluminium (Al) foil in order to collect fibres. The high-voltage power supply linked the injection syringe and the collector. During the experiment process, the sol was added to the injection syringe and then ejected with a voltage of 20 kV. The distance between the collector and the syringe needle point was 10 cm, and the injection pump velocity was 0.5 ml/h.

The phase of the PVP-precursor fibres was analysed by PANalytical X'Pert Pro MPD X-ray diffraction with Cu Kα radiation, and the tube voltage was 40 kV, the tube current was 40 mA, and the scanning speed was 4°C/min. The morphology of the fibres was observed by a scanning electron microscope (FEI Quanta 200, The Netherlands) with an acceleration voltage of 20 kV. The thermoanalysis proceeded using a thermogravimetric analyser (TGA Q50) (heating rate: 20°C/min, gas: N_2) and a differential scanning calorimeter (DSC204F1) (heating rate: 10°C/min, crucible: Al dish). The Fourier transform infrared (FTIR) analysis was conducted using a Spectrum100 Fourier infrared spectrometer (preforming: KBr).

3. Results and discussion

3.1. Microstructure and phase analysis: Fig. 2 shows the scanning electron microscopy (SEM) images of the composite fibres and the fibres calcined at 550°C. From Fig. 2*a*, it can be seen that the fibres are continuous and there are not any bead knots and bonding between fibres. The surface of the PVP-precursor

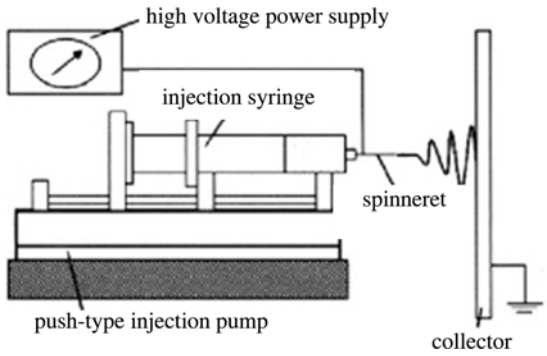

Figure 1 *Schematic diagram of electrostatic spinning device*

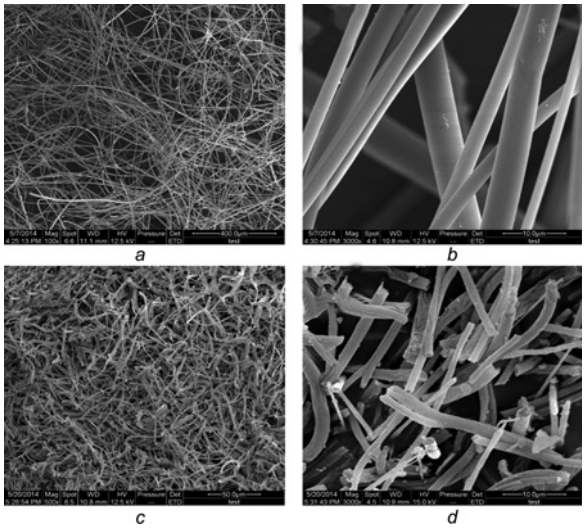

Figure 2 *SEM micrographs of PVP-processor fibers, and fibres calcined at 550°C*
a, *b* SEM micrographs of PVP-precursor fibres
c, *d* Fibres calcined at 550°C

composite fibres (Fig. 2*b*) is very smooth, which is attributed to the very fine particles or the amorphous nature of the composite fibres of the PVP-precursor [14].

Fig. 3 shows the X-ray diffraction (XRD) patterns of the compound PVP-precursor fibres. There is only one characteristic peak (2θ is about 23°), which proves the amorphous structure of the PVP-precursor fibres. Meanwhile, the fibre diameter is not very uniform, due to the change of air humidity and temperature during the process of electro-spinning. After being calcined at

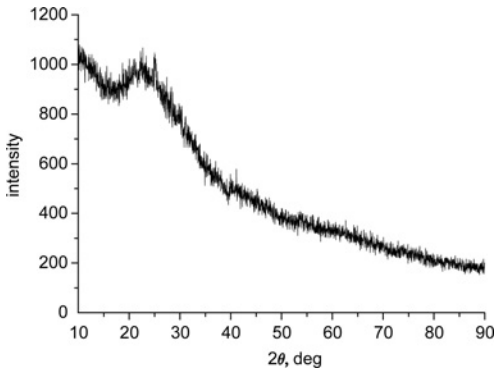

Figure 3 *XRD pattern of PVP-precursor fibres*

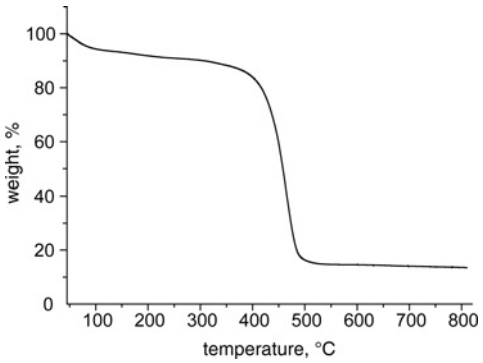

Figure 4 *TG curve of PVP-precursor fibres*

550°C, the target fibres were obtained. In Figs. 2*c* and *d*, the fibres show a decrease in diameter and shorter length. The obtained fibres were 500–3000 nm in diameter. As the PVP in the fibre is decomposed with the diameter reduction of the fibre, the continuous microstructure of the fibre is no longer maintained and the surface of the fibres become rough.

3.2. Thermoanalysis: The thermogravimetric (TG) curve of precursor fibres of the PVP precursor (Fig. 4) contains three stages relating to the fibres' weight loss. The first stage is between 45 and 100°C, and there is about 6% of the weight loss, which is attributed to the volatilisation of residual solvent – water in the fibres; the second stage presents ~8% of the weight loss from 100 to 380°C, which appears to be attributable to the PVP's part decomposition and weightlessness of crystallisation water in the raw materials; the last part is mainly the decomposition of PVP to generate 69% of the weight loss from 380 to 530°C. Above 530°C, the TG curve almost remains the same. It can be inferred that the instability of the PVP-precursor fibre occurs below 530°C. Fig. 4 shows the total 83% of the weight loss, and when the temperature reaches 530°C, PVP is degraded completely.

Fig. 5 shows the SEM image and the energy-dispersive X-ray spectroscopy (EDS) result of the residue black matter after the TG experiment. The SEM image shows a black mixture like ash and the mesh structure of class skeleton space. The black mixture like ash may be residue carbon and generated ZrO_2, which cover the graphitised carbon network structure and composite fibres to prevent being burned-off. Hence, the TG product contains plenty of C elements. It can form the basic skeleton of the carbon structure in the process of the pyrolysis PVP precursor. With the pyrolysis temperature increasing, the carbon structure merges and is rearranged further through thermal poly-condensation reaction, then gradually turns into a network structure of graphitised carbon.

Fig. 6 presents the differential scanning calorimetry (DSC) curve of the PVP-precursor fibres. There are primarily five peaks. The endothermic peak at 110°C could be attributed to the loss of the absorbed water and trapped solvent (water) from the PVP-precursor fibres. The two exothermic peaks at about 182 and

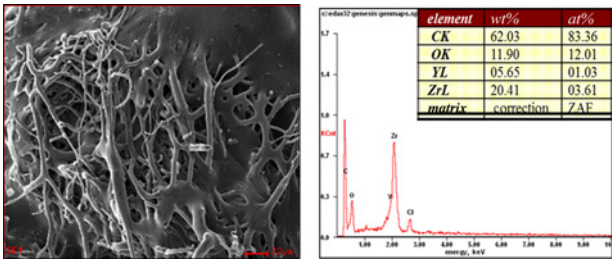

Figure 5 *SEM micrograph and EDS result of TG product*

doi: 10.1049/mnl.2014.0566

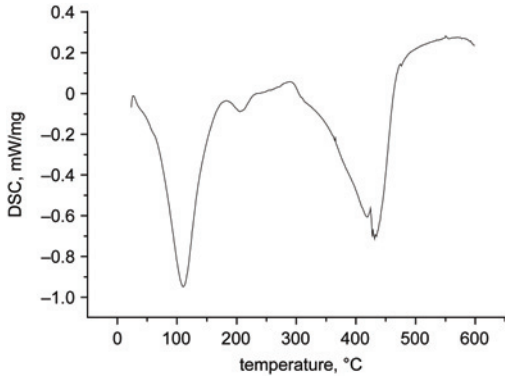

Figure 6 *DSC curve of PVP-precursor fibres*

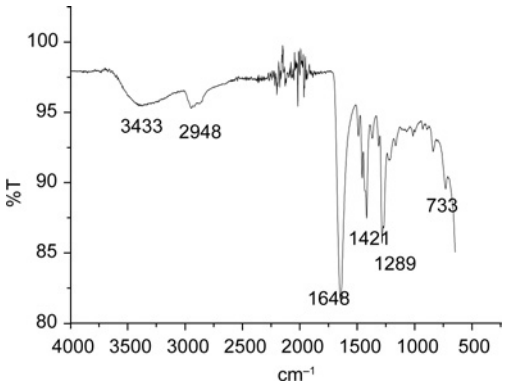

Figure 7 *FTIR analysis curve of PVP-precursor fibres*

290°C in the DSC curve correspond to the decomposition of PVP, and the endothermic peak at 205°C is due to the loss of crystal water from $Y(NO_3)_3{\cdot}6H_2O$ and $ZrOCl_2{\cdot}8H_2O$. The endothermic peaks at 420–434°C show that the amorphous ZrO_2 undergoes crystallisation. Combining Figs. 4 and 6, it can be concluded that the ZrO_2 fibres can be obtained when PVP-precursor fibres are calcined above 530°C through dehydration, oxidation decomposition and phase transition.

3.3. FTIR analysis: PVP-precursor fibres were qualitatively analysed by IR spectroscopy. The result is shown in Fig. 7. A strong broad band is seen at 3433 cm^{-1}, indicating the existence of O–H in the PVP-precursor fibres. The characteristic absorption bands at 2948 and 1421 cm^{-1} belong to the stretching vibration of C–H. The characteristic absorption peak of stretching vibration at 1648 cm^{-1} is of C = O and at 1289 cm^{-1} the characteristic absorption peak of stretching vibration is of C–N or C–O. Meanwhile, a weak peak is seen at 733 cm^{-1}, which is caused by the vibration of Y–O. Above 3800 cm^{-1}, the absorption peaks disappeared, proving that the PVP is degraded completely, which is the same as the TG results.

3.4. Synthetic mechanism of ZrO_2 fibres: Zirconium salts in an aqueous solution comprise two processes: hydrolysis and poly-condensation. When $ZrOCl_2{\cdot}8H_2O$ is dissolved in water, Zr^{4+} and Cl^- will not produce hydrolytic polymerisation reaction. The Zr^{4+} ion can be in coordination with H_2O or OH^- to mainly create a tetramer [15]. Meanwhile, the tetramer will be further polymerised to form a polymer. At the same time, active hydroxyl groups can be produced in the poly-condensation reaction process. Hence, PVP molecules evenly dispersed around the polymer of Zr atoms by hydrogen bonding. Then, this structure undergoes further poly-condensation and crosslinking to form the network polymer molecular, which is namely the sol.

During the electrostatic spinning process, the sol is treated under the effect of electrostatic repulsive force and Coulomb force to generate PVP composite fibres. The target ZrO_2 fibres are obtained after the PVP composite fibres are subjected to heat treatment. The heat treatment process includes a pyrolysis process at low temperatures and a crystallisation process at high temperatures. The pyrolysis decomposition process mainly consists of organic composition and moisture evaporation, and the crystallisation process at high temperatures is mainly the crystallisation of ZrO_2. It can form the basic skeleton of the carbon structure at the beginning of the process of the pyrolysis PVP precursor. With the pyrolysis temperature increasing, the carbon structure merges and is rearranged further through thermal poly-condensation reaction, then gradually turns into the graphitised carbon network structure. At the same time, small molecules of water will evaporate slowly. At this stage the heating rate should not be too fast; otherwise, the dehydration of organic matter decomposition will lead to many holes and cracks. Along with the pyrolysis process of PVP molecules, zirconium tetramer begins to dehydrate because of further poly-condensation. At this very moment, crystal nucleus begin to form. As temperature increases, the degree of supersaturation and the number of crystal nuclei also increases. When reaching the conditions of the nucleus growing up, namely the degree of supersaturation and number of crystal nucleus are enough, crystal nucleus begins to grow up increasingly. Owing to the grain growth, the amorphous ZrO_2 turns crystalline. Hence, ZrO_2 fibres are formed.

4. Conclusion: ZrO_2 fibres by Y-doping were successfully prepared using the sol–gel method and an electrostatic spinning method. The diameter of the fibres are in the range of 500–3000 nm. The results of thermoanalysis indicate that PVP-precursor fibres should go through obvious dehydration, oxidation decomposition and phase transition processes before ZrO_2 nanofibres are synthesised. It can form the basic skeleton of the carbon structure at the beginning of the process of the pyrolysis PVP-precursor. With the increase in pyrolysis temperature, the carbon structure merges and is rearranged further through thermal poly-condensation reaction, and then gradually turns into graphitised carbon network structures.

5. Acknowledgments: This work was financially supported by the National Basic Research Program of China (973 Program) (no. 2011CB013404), the National Natural Science Foundation of China (nos. 51275105, 51375106) and the Fundamental Research Funds for the Central Universities (nos. HEUCF20130910003, 201403017).

6 References

[1] Liu H.Y., Hou X.Q., Wang X.Q., *ET AL.*: 'Fabrication of high–strength continuous zirconia fibers and their formation mechanism study', *J. Am. Ceram. Soc.*, 2004, **87**, (12), pp. 2237–2241

[2] Wang S., Li Y., Zhang X.: 'Influence of the microstructure evolution of ZrO_2 fiber on the fracture toughness of ZrB_2–SiC nanocomposite ceramics', *Mater. Des.*, 2013, **49**, pp. 808–813

[3] Park K., Vasilos T.: 'Microstructure and thermal shock resistance of Al_2O_3 fiber/ZrO_2 and SiC fiber/ZrO2 composites fabricated by hot pressing', *J. Mater. Sci.*, 1999, **34**, (12), pp. 2837–2842

[4] Bugaeva A.Y., Loukhina I.V., Belyi V.A., Dudkin B.N.: 'Ceric oxide effect on heat-induced transformations of zirconium oxide microfibers prepared by impregnation of cotton fiber', *Russ. J. Gen. Chem.*, 2014, **84**, (2), pp. 190–193

[5] Yu G., Zhu L.Y., Wang X.Q., *ET AL.*: 'Fabrication of zirconia mesoporous fibers by using polyorganozirconium compound as precursor', *Micropor. Mesopor. Mater.*, 2009, **119**, (1), pp. 230–236

[6] Xu P.P., Wang X.F., Fu S.D., Jian F.X.: 'Preparation of zirconia-yttrium fibres from steady precursor by sol-gel technique', *Adv. Mater. Res.*, 2012, **535**, pp. 2087–2091

[7] Sun G., Du X., Zhang M., Zhou C., Chen J., Liu F.: 'Fabrication of zirconia fibers by a sol–gel combined rotational centrifugal spinning technique', *Trans. Indian Ceram. Soc.*, 2014, **73**, (3), pp. 228–232
[8] Azad A.M.: 'Fabrication of yttria-stabilized zirconia nano fibers by electro spinning', *Mater. Lett.*, 2006, **60**, (1), pp. 67–72
[9] Shao C.L., Guan H.Y., Liu Y.C., Gong J., Yu N., Yang X.H. : 'A novel method for making ZrO_2 nanofibres via an electro spinning technique', *J. Cryst. Growth*, 2004, **267**, (1), pp. 380–384
[10] Huang Z.M., Zhang Y.Z., Kotaki M., Ramakrishna S.: 'A review on polymer nano fibers by electro spinning and their applications in nano-composites', *Compos. Sci. Technol.*, 2003, **63**, (15), pp. 2223–2253
[11] Watthanaarun J., Pavarajarn V., Supaphol P.: 'Titanium (IV) oxide nano fibers by combined sol–gel and electro spinning techniques: preliminary report on effects of preparation conditions and secondary metal dopant', *Sci. Technol. Adv. Mater.*, 2005, **6**, (3), pp. 240–245
[12] Li D., McCann J.T., Xia Y., Marquez M.: 'Electrospinning: a simple and versatile technique for producing ceramic nano fibers and nano-tubes', *J. Am. Ceram. Soc.*, 2006, **89**, (6), pp. 1861–1869
[13] Franco P.Q., João C.F.C., Silva J.C., Borges J.P.: 'Electrospun hydroxyapatite fibers from a simple sol–gel system', *Mater. Lett.*, 2012, **67**, (1), pp. 233–236
[14] Li J.Y., Dai H., Li Q., Zhong X.H., Ma X.F., Meng J., Cao X.Q.: 'Lanthanum zirconate nano fibers with high sintering-resistance', *Mater. Sci. Eng., B*, 2006, **133**, (1), pp. 209–212
[15] Matsui K., Ohgai M.: 'Formation mechanism of hydrous–zirconia particles produced by hydrolysis of $ZrOCl_2$ solutions: II', *J. Am. Ceram. Soc.*, 2000, **83**, (6), pp. 1386–1392

doi: 10.1049/mnl.2014.0566